PHYSICAL REVIEW LETTERS

Ground States and Defect Energies of the Two-Dimensional *XY* Spin Glass from a Quasiexact Algorithm

Martin Weigel* and Michel J. P. Gingras

Department of Physics, University of Waterloo, Waterloo, Ontario, N2L 3G1, Canada
(Received 23 October 2005; published 9 March 2006)

We employ a novel algorithm using a quasiexact embedded-cluster matching technique as minimization method within a genetic algorithm to reliably obtain numerically exact ground states of the Edwards-Anderson *XY* spin-glass model with bimodal coupling distribution for square lattices of up to 28×28 spins. Contrary to previous conjectures, the ground state of each disorder replica is nondegenerate up to a global O(2) rotation. The scaling of spin and chiral defect energies induced by applying several different sets of boundary conditions exhibits strong crossover effects. This suggests that previous calculations have yielded results far from the asymptotic regime. The novel algorithm and the aspect-ratio scaling technique consistently give $\theta_s = -0.308(30)$ and $\theta_c = -0.114(16)$ for the spin and chiral stiffness exponents, respectively.

Since the suggestion by Edwards and Anderson (EA) to capture the essence of spin-glass behavior in a class of simple lattice models 30 years ago [1], the quest for their understanding has spurred an enormous research effort [2]. EA considered the Hamiltonian

$$\mathcal{H} = -\sum_{\langle ij \rangle} J_{ij} \mathbf{S}_i \cdot \mathbf{S}_j, \qquad (1)$$

with O(n) spins $\mathbf{S}_i$ on a regular lattice with quenched, random, and frustrated nearest-neighbor interactions J_{ij}. Although substantial progress has been made in recent years in understanding Ising and vector spin glasses in finite dimensions D, mostly by the development and application of sophisticated numerical techniques, we still lack an undisputed theory of the spin-glass phase [2]. Because of its relative simplicity, by far the most work has been devoted to the Ising spin glass [2]. However, much less advance has been made on models with continuous spins which are often more relevant to real materials [2].

The properties of the spin-glass phase in the EA model are described by a scaling theory of the associated zero-temperature fixed point [3]. The corresponding renormalization-group (RG) picture considers the scaling of the width of the distribution of random couplings, $P_L(J_{ij})$, with the coarse-graining length scale L, $J(L) \sim J L^{\theta_s}$, defining the spin stiffness exponent θ_s. Depending on whether $\theta_s > 0$ or $\theta_s < 0$, the spin-glass phase is stable or unstable against thermal fluctuations, respectively. Following a suggestion by Banavar *et al.* and McMillan [4], the scaling of $J(L)$ can be inferred from monitoring the dependence of the energy of droplet or domain-wall excitations induced by a change of boundary conditions (BCs), giving rise to the name "domain-wall RG" (DWRG) method. For cases where $\theta_s < 0$, and thus the spin-glass transition temperature $T_g = 0$, such as for the EA Ising model in two dimensions (2D) [2], θ_s also determines the critical behavior with the spin-glass correlation length

diverging as $\xi \sim T^{-\nu_s}$ for $T \downarrow 0$, where $\nu_s = -1/\theta_s$ [3]. Furthermore, unless exact ground-state degeneracies occur, as for the Ising model with bimodal $P(J_{ij})$ [3], θ_s is the only nontrivial exponent, while the critical exponent η is simply $2 - D$ when $\theta_s < 0$ [3]. Consequently, 2D models offer a crucial test bench for our understanding of spin glasses at low temperatures.

Twenty years of research since the original DWRG work of Morris *et al.* [5] have not been able to settle a number of persistent controversies concerning the ground-state properties of the 2D *XY* spin glass. Firstly, it has been suggested that the ground state may possess nontrivial extensive degeneracies when $P(J_{ij})$ is a discrete bimodal distribution [6–8]. Secondly, it was realized early [9] that the rotational symmetry of the *XY* spin glass is accompanied by a $\mathbb{Z}_2$ symmetry originating from the difference between proper and improper O(n) rotations [10]. It has been suggested that the resulting Ising-like *chirality* variables may decouple from the rotational degrees of freedom, leading to different critical behavior for the spin and chiral variables [11]. For $D = 2$, where $T_g = 0$, this would entail distinct spin and chiral stiffness exponents, $\theta_s = -1/\nu_s$ and $\theta_c = -1/\nu_c$, respectively. Finally, and most noteworthy, previous Monte Carlo (MC) [6] and DWRG studies [5,12,13] have yielded rather inconsistent values for θ_s. This might be partly explained by the difficulty in obtaining ground-state configurations of the model. Parallel alignment of the spins to their local molecular fields $\mathbf{h}_i = \sum_j J_{ij} \mathbf{S}_j$ is a necessary condition for metastability of the system (1). However, due to the broad spectrum of an exponential number of metastable states, the resulting commonly used [5,12] iterative spin-quench algorithm [14] almost never yields a ground-state configuration. Additionally, experience with the simpler 2D Ising case shows that finite-size corrections as well as the dependence on the chosen pair of boundary conditions are generically large [15,16]. Hence it seems likely that the observed inconsis-

tencies for the *XY* model to date are due to system-size restrictions, improper finite-size scaling analyses, and limitations in probing the true ground-state behavior.

Toulouse noted that the ground-state problem for the 2D Ising spin glass on a planar graph can be transformed to a minimization problem for the total length of energy strings on the dual lattice, connecting pairs of *frustrated plaquettes*, i.e., graph faces containing an odd number of negative bonds [17,18]. It was later realized [19] that this constitutes a *minimum-weight perfect matching problem*, which is well-known in graph theory and can be solved in polynomial time, such that the ground state of large 2D Ising spin-glass systems can be found exactly. In contrast, the *XY* model ground-state problem is seemingly not polynomial. However, in this Letter we propose that a partial solution can be found in polynomial time by an embedding of Ising variables into the continuous spins, allowing us to obtain new results addressing the controversies alluded to above. This embedding is achieved by choosing a random direction r in spin space to decompose the spins as $S_i = S_i^{\parallel} + S_i^{\perp} = (S_i \cdot r)r + S_i^{\perp}$. A reflection $R_i(r)$ of S_i along the plane defined by r maps $S_i^{\parallel} \to -S_i^{\parallel}$ and $S_i^{\perp} \to S_i^{\perp}$. Hence, with respect to these local reflections the Hamiltonian (1) decomposes as $\mathcal{H} = \mathcal{H}^{r,\parallel} + \mathcal{H}^{r,\perp}$ with $\mathcal{H}^{r,\parallel} = -\sum_{\langle i,j \rangle} \tilde{J}_{ij}^r \, \epsilon_i^r \epsilon_j^r$, and

$$\tilde{J}_{ij}^r = J_{ij}|S_i \cdot r||S_j \cdot r|, \qquad \epsilon_i^r = \mathrm{sgn}(S_i \cdot r). \quad (2)$$

Thus, since the $R_i(r)$ merely induce an inversion $\epsilon_i^r \to -\epsilon_i^r$, the O($n$) model Hamiltonian (1) is formally identified with that of an Ising model, if spin changes are restricted to the reflections $R_i(r)$. One can then proceed as follows: decompose the O(n) spins S_i with respect to r and find the corresponding Ising ground state using the matching technique [19]. This corresponds to a reflection of some of the S_i and thus a new valid O(n) model configuration. With $\mathcal{H}^{r,\perp}$ being invariant, this embedded ground-state search decreases the total energy of (1) or leaves it constant. The full O(n) symmetry can then be statistically recovered by sequential minimizations for a series $r_1, r_2, r_3, \ldots$ of random directions. We call this procedure "embedded matching." If (1) is in a ground state, all the embedded Ising systems must be in (one of) their respective ground state(s) as well. However, stationarity of the process of successive embedded Ising-like matching minimization steps does not guarantee global minimum energy for the system (1) [20]. Thus, the corresponding artificial dynamics exhibits metastability, however with far less metastable states than the local spin-quench method [20]. For further improvement, and to find true ground states with high reliability, the embedded-matching procedure is inserted as a minimization step into a specially tailored genetic algorithm [20]. Generally speaking, in a genetic algorithm a population of $\mathcal{N}_0$ candidate ground-state configurations is being iteratively optimized by mixing or "crossing over" the "genetic material" of different candidate ground states and

eliminating the less well adapted instances [21]. To achieve reasonable performance, this crossover operation has to be chosen appropriately. Specifically, we are guided by the direct (visual) inspection of the spin configurations from different metastable states obtained by the embedded-matching technique. There, due to the local spin rigidity, the predominant differences consist of (proper or improper) O(n) rotations of rigid domains. Hence, to preserve the high level of optimization already obtained *inside* of domains at intermediate stages of the evolution, new offspring configurations are produced by randomly exchanging these (automatically determined) domains instead of single spins between the parent replica. Full details of the algorithm will be presented elsewhere [20] (for a related method for the Ising case see Ref. [22]). This "genetic embedded-matching" (GEM) approach works very reliably already for small $\mathcal{N}_0$ as shown in Fig. 1. There, we compare the histograms of energies of metastable states found from statistically independent runs for the same $\pm J$ disorder configuration $\{J_{ij}\}$ of a 24×24 system using either the simple spin-quench approach [14], the simulated annealing method, or the GEM technique. The first two methods give broad distributions of energies, whereas on this scale, the GEM always seems to yield the same energy, which is clearly below the range of energies regularly found by the other approaches. Only on examining the histograms at much higher resolution, do the GEM data get resolved into a small series of sharp peaks, corresponding to different energy levels, cf. the upper inset of Fig. 1. On increasing $\mathcal{N}_0$ from $\mathcal{N}_0 = 64$, chosen for the runs in Fig. 1, to $\mathcal{N}_0 = 256$, the peaks displayed in the inset all
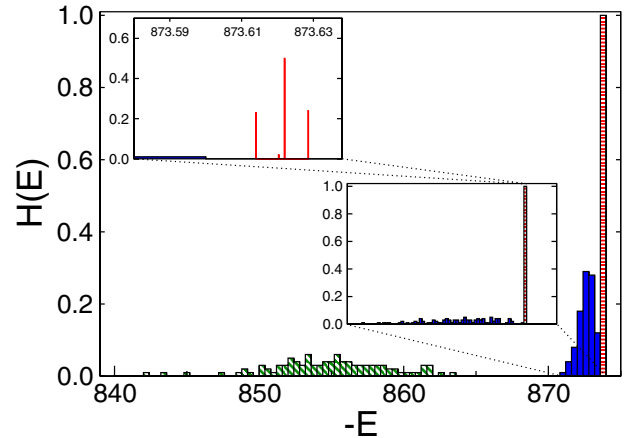

FIG. 1 (color online).   Histogram $H(E)$ of minimum energies obtained from repeated runs using the spin-quench method [diagonally hatched bars (green online)], simulated annealing [solid bars (blue online)] and the genetic embedded-matching technique [horizontally hatched bars (red online)] for a *single* disorder realization $\{J_{ij}\}$ of system size 24×24. The insets show blowups of the region around the true ground state. The genetic matching was run here with a small population of $\mathcal{N}_0 = 64$ replica; for $\mathcal{N}_0 = 256$, all runs converge to the rightmost bar of the top inset.

collapse onto the peak of lowest energy on the right, corresponding to the true ground state.

As a first result we find, perhaps surprisingly, that the ground states thus obtained for a given bimodal disorder realization are not only identical in energy up to machine precision (15 digits) between statistically independent runs, but the final optimized spin configurations themselves are trivially related to each other by *global* O(n) transformations [20]. In other words, the ground states are unique and, in contrast to the bimodal Ising model [2], no accidental degeneracies occur. Hence, after averaging over disorder, the ground state is ordered and the spin correlation function is constant, implying $\eta = 0$ [3]. This is in contrast to indications by MC simulations [6,7] and Migdal-Kadanoff calculations [8], which presumably did not probe the true ground-state behavior.

Strong dependence of the domain-wall scaling on the choice of BCs has been observed for the Ising spin glass [15,23]. Further complications arise for the *XY* case due to the simultaneous presence of continuous (spin) and discrete (chiral) symmetries: for both periodic (P) and anti-periodic (AP) BCs, domain walls might be forced into the system due to the periodicity, such that the P-AP energy difference does not directly capture the energy of single walls. In Ref. [13], it was attempted to alleviate this problem by introducing a twist along the boundary, which is included in the optimization process to yield "optimum twist" BCs. Nevertheless, additional *chiral* domain walls might still occur in the measurements of spin domain walls. In fact, it has been found that for (quasi) one-dimensional *XY* systems *both* P-AP and reflective BCs asymptotically probe the chiral excitations [24]. These problems, resulting from a periodic constraint, can be circumvented by applying open and domain-wall (O-DW) BCs. There, one ensures the insertion of single domain walls by comparing the ground state of a system with open BCs to one where the relative orientations of spins linked across the boundary are either rotated by an angle π for spin domain walls or, for chiral domain walls, are reflected along an arbitrary but common axis by introducing very strong bonds across the boundary [20,25]. In addition, and for comparison, we consider P-AP and random-antirandom (R-AR) BCs as well, the latter fixing the boundary spins in random relative orientations for one ground-state computation (R) and in relatively π-rotated orientations for AR BCs. In all cases, the edges with unaltered BCs are left open. Ground states are computed for systems of up to 28×28 spins, using 5000 disorder realizations with $J_{ij} = \pm J$ at equal proportions. Figure 2 shows the results for the three sets of BCs together with fits of the asymptotically expected form $[|\Delta E|]_J \sim L^\theta$ to the data, where $[\cdot]_J$ denotes the average over disorder. The results for P-AP BCs show a pronounced crossover from $\theta = -0.724(21)$ for $L \leq 12$ to $\theta = -0.433(26)$ for $L \geq 16$, the first value being compatible with the "random twist" data of Ref. [13] drawn for comparison ($\theta_s =$
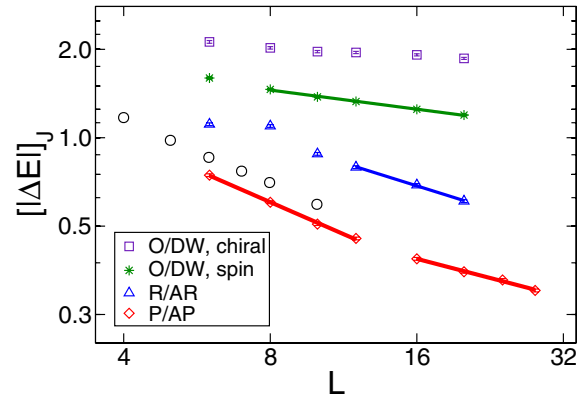

FIG. 2 (color online).   Log-log plot of the average domain-wall energies $[|\Delta E|]_J$ for three sets of boundary conditions on square lattices as a function of system size L. The lines are fits of the form $[|\Delta E|]_J \sim L^\theta$ to the data. The black circles show the random twist result of Ref. [13] for comparison. Some data sets have been shifted vertically for better distinction.

-0.76), which are representative of previous results for P-AP BCs and small system sizes [12]. On the other hand, $\theta = -0.433(26)$ is closer to the optimum twist result of Ref. [13], designed to alleviate the problem of trapped domain walls. Note that the apparent crossover length is compatible with the length below which no metastability occurs and the system behaves like a spherical spin glass [5,26]. The other BCs yield less negative values already for smaller system sizes, resulting in $\theta_s = -0.519(30)$ for the R-AR combination and $\theta_s = -0.207(12)$ for the O-DW BCs. The scaling of the chiral domain-wall energies from O-DW boundaries yields an only slightly negative value $\theta_c = -0.090(23)$.

The above usage of multiple pairs of BCs reveals the presence of pronounced finite-size corrections, even for the already larger system sizes considered here compared to previous studies [5,12,13]. Part of these corrections are due to irrelevant scaling fields and subleading analytical terms, giving rise to the general form $[|\Delta E|]_J(L) = AL^\theta + BL^{-\omega} + C/L + D/L^2 + \cdots$. For a proper resolution of these contributions, much larger system sizes, out of the reach of current numerical methods, would be necessary. Thus, we have to restrict ourselves here to a successive omission of data points from the small-L side to extrapolate towards $L \to \infty$. Additional corrections, however, result from the dependence on the considered pair of BCs. For the Ising system, it has been argued that such corrections might be suppressed by considering $L \times M$ systems (the change of BCs happening along the edges of length L) with aspect ratios $R \equiv M/L \neq 1$ [23]. Neglecting for the time being the corrections listed above, the asymptotic scaling of defect energies should then follow the form $[|\Delta E|]_J(L, M) = L^\theta F(R)$ with some scaling function F. In general, $F(R)$ depends on the BCs applied [23]. However, there is no dependence on BCs for one-dimensional systems [3,24], such that $F(R)$ is independent
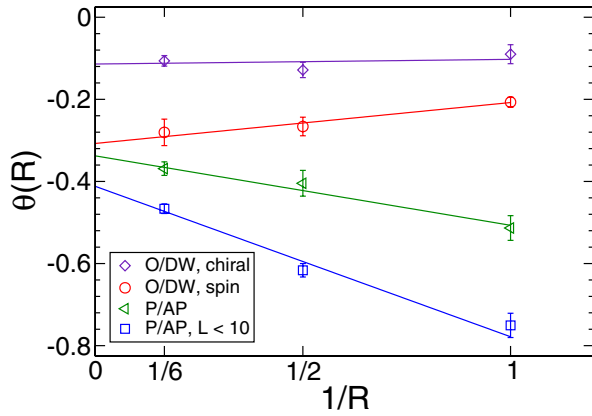
FIG. 3 (color online). Aspect-ratio scaling of the stiffness exponents θ_s and θ_c for aspect ratios $R = 1$, 2, and 6 as a function of $1/R$. The bottom data set corresponds to fits for the fixed R data restricted to $L \leq 10$ (see text). The solid lines show fits of the functional form $\theta(R) = \theta(R = \infty) + A_R/R$ to the data.

of BCs in the limit $R \to \infty$ and the corresponding corrections should disappear as more and more elongated systems are being considered. To investigate this, we determined the ground states of 5000 disorder replica and $L = 4, 6, \ldots, 16$ for $R = 2$ and $L = 3, 4, \ldots, 9$ for $R = 6$ in addition to the data for the square systems ($R = 1$) for the different sets of BCs. Figure 3 shows the estimated stiffness exponents as a function of R for P-AP and O-DW BCs together with fits of the functional form $\theta(R) = \theta(R = \infty) + A_R/R$ to the data, which is inspired by the results for the Ising case [15,23]. The scaling corrections at *fixed R* listed above are taken into account by including only the largest lattice sizes in the fits of $[|\Delta E|]_J \sim L^\theta$. For comparison, the bottom data set of Fig. 3 shows the results from including a fixed range of sizes $L \leq 10$ for each aspect ratio R, thus admixing the two correction effects. The fits result in consistent asymptotic estimates of the spin stiffness exponent of $\theta_s(R = \infty) = -0.338(20)$ from P-AP BCs and of $\theta_s(R = \infty) = -0.308(30)$ from O-DW BCs, indicating that the asymptotic regime is indeed being probed. The chiral exponent θ_c, on the other hand, depends only weakly on R, and the asymptotic estimate $\theta_c(R = \infty) = -0.114(16)$ is clearly different from θ_s.

In conclusion, we have developed a novel quasiexact algorithm to determine the ground state of 2D O(n) spin glasses. Considering for specificity the 2D *XY* spin-glass model with bimodal distribution of random exchange couplings J_{ij}, we have shown from computations for relatively large systems sizes that, as argued in Ref. [13], defect-wall calculations from P-AP BCs indeed suffer from large finite-size corrections due to the periodic constraint. Using aspect-ratio scaling, however, they are found to asymptotically yield the same scaling behavior as the less ambiguous O-DW BCs showing less pronounced corrections, and we quote the latter result as our final estimate, $\theta_s = -0.308(30)$. This might be compared with $\theta_s \approx -0.28$ for the 2D Ising case with *Gaussian* coupling dis-

tribution [15,25]. The chiral exponent is found to be $\theta_c = -0.114(16)$, clearly different from the spin exponent θ_s, indicating spin-chirality decoupling, and close to the value $\theta_s = 0$ found for the 2D bimodal Ising spin glass [25]. Yet, no exact degeneracies as occurring in the latter case are found here. It would be very interesting to see whether the *XY* spin glass with Gaussian couplings shows a different behavior than the $\pm J$ case considered here. The 2D Heisenberg spin glass is another exciting problem to explore.

*Present address: Department of Mathematics, Heriot-Watt University, Edinburgh, EH14 4AS, United Kingdom.
[1] S. F. Edwards and P. W. Anderson, J. Phys. F **5**, 965 (1975); **6**, 1927 (1976).
[2] N. Kawashima and H. Rieger, in *Frustrated Spin Systems*, edited by H. T. Diep (World Scientific, Singapore, 2005).
[3] A. J. Bray and M. A. Moore, in *Heidelberg Colloquium on Glassy Dynamics*, edited by J. L. van Hemmen and I. Morgenstern (Springer, Heidelberg, 1987).
[4] J. R. Banavar and M. Cieplak, Phys. Rev. Lett. **48**, 832 (1982); W. L. McMillan, Phys. Rev. B **29**, 4026 (1984).
[5] B. W. Morris *et al.*, J. Phys. C **19**, 1157 (1986).
[6] S. Jain and A. P. Young, J. Phys. C **19**, 3913 (1986).
[7] P. Ray and M. A. Moore, Phys. Rev. B **45**, 5361 (1992).
[8] M. J. P. Gingras, Phys. Rev. B **46**, 14 900 (1992).
[9] G. Toulouse, Phys. Rep. **49**, 267 (1979).
[10] J. Villain, J. Phys. C **10**, 4793 (1977).
[11] H. Kawamura and M. Tanemura, Phys. Rev. B **36**, 7177 (1987).
[12] J. Maucourt and D. R. Grempel, Phys. Rev. Lett. **80**, 770 (1998).
[13] J. M. Kosterlitz and N. Akino, Phys. Rev. Lett. **82**, 4094 (1999).
[14] L. R. Walker and R. E. Walstedt, Phys. Rev. B **22**, 3816 (1980).
[15] A. K. Hartmann *et al.*, Phys. Rev. B **66**, 224401 (2002).
[16] C. Amoruso *et al.*, Phys. Rev. Lett. **91**, 087201 (2003).
[17] A. K. Hartmann and H. Rieger, *Optimization Algorithms in Physics* (Wiley, Berlin, 2002).
[18] G. Toulouse, Commun. Phys. **2**, 115 (1977).
[19] I. Bieche *et al.*, J. Phys. A **13**, 2553 (1980).
[20] M. Weigel (to be published).
[21] K. F. Pál, Physica (Amsterdam) **223A**, 283 (1996); A. K. Hartmann, Europhys. Lett. **40**, 429 (1997).
[22] A. K. Hartmann, Physica (Amsterdam) **224A**, 480 (1996).
[23] A. C. Carter, A. J. Bray, and M. A. Moore, Phys. Rev. Lett. **88**, 077201 (2002).
[24] M. J. Thill, M. Ney-Nifle, and H. J. Hilhorst, J. Phys. A **28**, 4285 (1995).
[25] A. K. Hartmann and A. P. Young, Phys. Rev. B **64**, 180404 (2001).
[26] L. W. Lee and A. P. Young, Phys. Rev. E **72**, 036124 (2005).